Study of full band gaps and propagation of acoustic waves in two-dimensional piezoelectric phononic plates

Jin-Chen Hsu and Tsung-Tsong Wu

Institute of Applied Mechanics, National Taiwan University, No. 1, Sec. 4, Roosevelt Road, 106 Taipei, Taiwan

hsu@ndt.iam.ntu.edu.tw

In this study, we investigate the band-gap and propagation properties of acoustic waves in two-dimensional (2D) phononic crystal plates that consist of piezoelectric material by employing a revised full three-dimensional (3D) plane wave expansion (PWE) method and finite element method (FEM). The considered structures are periodic air-hole array in a zinc oxide plate. To apply the PWE method efficiently and to the piezoelectric solids, the equations governing the piezoelectric wave propagation are considered, and Fourier series expansions are performed not only in the 2D periodic plane, but also in the thickness direction for an imaginary 3D periodic structure by stacking the phononic-crystal plates and uniform vacuum layers alternatively, In the investigated piezoelectric phononic plates, large full band gaps are found. On the other hand, analyses by FEM using Bloch periodic boundary conditions is also employed to compare the results from the PWE method and to serve as a numerical tool for a more detailed study. Effects of lattices and thickness of the phononic plate on the full band gaps are discussed as well.

1   Introduction

In recent years, there has been an increasing interest in studying the properties of acoustic wave propagation in the composite materials, called phononic crystals (PCs), whose mass densities and elastic coefficients are periodically modulated in space. The interest in these materials mainly arises from that they can give rise to complete acoustic stop bands, which are analogous to the photonic band gaps for optical or electromagnetic waves in photonic crystals and may find many promising applications to engineering such as acoustic wave guiding, filtering, and vibration shielding [1, 2]. In addition to those phononic structures dealing with the bulk acoustic modes that travel in the interior of the medium and the acoustic modes localized near a truncated free surface of the two-dimensional periodic plane of the structure [3-5], very recent studies show that another worthwhile category of phononic-crystal structures would be the periodic plates of finite thickness whereby the Lamb waves can propagate in [6-9]. On the other hand, it is worth noting that Lamb modes have been important in a variety of applications, such as characterization of elastic properties of thin films, resonators, and sensing applications. For periodic plate structures, some released experiments [6] and theoretical work [7, 8] have demonstrated the existence of directional and complete band gaps of Lamb waves, respectively; these demonstrations may also facilitate the usages of band-gap materials from those conducted by bulk and surface acoustic modes to the Lamb-wave modes in phononic plate structures. Moreover, Lamb waves are guided waves and well-confined in the thickness direction. As a result, the two-dimensional (2D) phononic plates can be expected to serve the same properties of a forbidden band for Lamb modes as a three-dimensional phononic crystal for bulk acoustic modes, in a much more unsophisticated way.

Among the existing studies, a lot of theoretical methods, for instance, plane wave expansion (PWE) method, multiple-scattering theory (MST), finite element method (FEM), and finite-difference time-domain (FDTD) method [10], have been successfully applied to analyze the bulk acoustic waves in infinite phononic crystals; however, it is not always a straight forward task to adapt these methods for phononic plate problems. Based on the classical plate theory and three-dimensional equations of motion with suitable boundary conditions, respectively, the PWE method is used to address the phononic plate problems [11, 12]. Applying Bloch theorem of a periodic medium to the FEM formulation, the frequency band structures of Lamb waves in phononic plate consisting of quartz inclusions arranged periodically in an epoxy host were calculated and analyzed [8]. Recently, the Mindlin's plate theory based PWE method has been developed to analyze the frequency band structures of lower-order Lamb modes in lower bands for 2D non-piezoelectric phononic plates [9]. As well as, a full 3D PWE method is modified by considering an imaginary 3D periodic layered structure to analyze the waves in phononic crystal plate [13, 14].

In this paper, we derive a full 3D PWE method for 2D phononic plate containing constituents with piezoelectricity. Similar to the idea by considering an imaginary 3D periodic layered structure in the Fourier expansion, the formulation of piezoelectric version is proposed. Moreover, FEM model is also applied to serve a more detailed study. The plate considered and studied is made of zinc oxide film with a periodic air-hole array.

2   Methods of Calculation

2.1   Plane wave expansion method

Consider a phononic crystal plate with thickness h as shown in Fig. 1, which is composed of an array of cylindrical inclusions A periodically filled in an infinite matrix B. Moreover, in order to apply the full 3D PWE method to phononic plates, the phononic plate is placed on a uniform layer C of thickness H that will be taken as a vacuum layer in the PWE calculation. Such a system is then assumed to be periodically stacked along the thickness direction (i.e., the z direction) to form an imaginary three-dimensional periodic structure. The period l along the z-direction is, therefore, $l=h+H$. As a result, the traction-free boundary conditions and continuity of the electric displacement at the up and down surfaces of the phononic plate are implicitly satisfied in the full 3D PWE formulation.
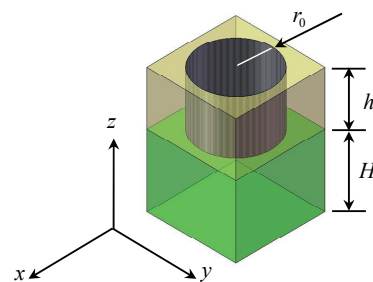
FIG. 1 Unit cell of an imaginary 3D periodic structure by stacking a phononic plate and a uniform layer in the PWE method.

The governing field equations of acoustic wave propagation in a piezoelectric solid are given by

$$\rho \ddot{u}_j = \frac{\partial}{\partial x_i}\left(c_{ijkl}\frac{\partial u_k}{\partial x_l} + e_{lij}\frac{\partial \phi}{\partial x_l}\right), \qquad (1)$$

$$0 = \frac{\partial}{\partial x_i}\left(e_{ikl}\frac{\partial u_k}{\partial x_l} - \varepsilon_{il}\frac{\partial \phi}{\partial x_l}\right), \qquad (2)$$

where u_j is the displacement and ϕ is the electric potential. ρ, c_{ijkl}, e_{ikl}, and ε_{ij} are position-dependent mass density, elastic stiffness, piezoelectric constants, and permittivity, respectively. Since the imaginary structure is 3D periodicity in space now, the displacements and electric potential satisfy the Bloch theorem that can be expressed as follows:

$$u_j = \sum_G A_G^j e^{i(G+k)\cdot r - i\omega t}, \qquad (3)$$

$$\phi = \sum_G A_G^4 e^{i(G+k)\cdot r - i\omega t}, \qquad (4)$$

where $\mathbf{k}=(k_x, k_y)$ is the Bloch wave vectors in the 2D first Brillouin zone, and $\mathbf{r}=(x, y, z)$ and $\mathbf{G}=(G_x, G_y, G_z)$ are 3D position vectors and reciprocal lattice vectors, respectively. Moreover, spatial distributions of the material properties can be expanded in the Fourier series, as

$$f(\mathbf{r}) = \sum_G f_G e^{iG\cdot r}, \qquad (5)$$

where the function f is any one of the position-dependent material properties. The Fourier coefficients of the material properties can be evaluated by the formula

$$f_G = V_c^{-1}\int_{V_c} f(\mathbf{r}) e^{-iG\cdot r} dV, \qquad (6)$$

where V_c is the volume of a unit cell of the imaginary 3D periodic structure. Substitution of Eqs. (3), (4), and (5) into Eqs. (1) and (2) leads to a linear system of equations in the matrix form:

$$\begin{pmatrix} L_{G,G'}^{11} & L_{G,G'}^{12} & L_{G,G'}^{13} & L_{G,G'}^{14} \\ L_{G,G'}^{21} & L_{G,G'}^{22} & L_{G,G'}^{23} & L_{G,G'}^{24} \\ L_{G,G'}^{31} & L_{G,G'}^{32} & L_{G,G'}^{33} & L_{G,G'}^{34} \\ L_{G,G'}^{41} & L_{G,G'}^{42} & L_{G,G'}^{43} & L_{G,G'}^{44} \end{pmatrix} \cdot \begin{pmatrix} A_{G,G'}^1 \\ A_{G,G'}^2 \\ A_{G,G'}^3 \\ A_{G,G'}^4 \end{pmatrix} \equiv \mathbf{L}\cdot\mathbf{A} = \mathbf{0} \quad (7)$$

Note that the summations of the reciprocal lattice vectors in Eqs. (3), (4), and (5) have to be truncated to obtain a finite-dimension square matrix **L**. In practicing the numerical calculations, the *z*-component of **G** is separated as $\mathbf{G}=(\mathbf{G}_\parallel, G_z)$, where $\mathbf{G}_\parallel$ is 2D a reciprocal lattice vector, dependent on the lattice symmetry of the phononic plate, and the *z* component of **G** is $G_z = 2n\pi / l$, $(n = 0, \pm 1, \pm 2, ...)$.

To give an explicit expression of the Fourier coefficient for the imaginary 3D structure, Eq. (6) can be rewritten as

$$f_G = l^{-1}f_C \cdot \int_{-H/2}^{H/2} e^{-iG_z z} dz +$$
$$l^{-1}f_{pc}(x,y)\cdot\left(\int_{H/2}^{l/2} e^{-iG_z z} dz + \int_{-l/2}^{-H/2} e^{-iG_z z} dz\right) \qquad (8)$$

In this form, we set the interval of the integration to integrate over one unit cells that is symmetric with respect to the *x-y* plane, which can avoid the algebraic operation of the complex numbers, and the function f_{pc} is the distribution of material properties in the 2D phononic-crystal plate. The final result is given by

$$f_G = f_C \cdot S_z(H/2) + (f_A - f_B)\cdot S_{xy}(r_0)\cdot\left(S_z(l/2) - S_z(H/2)\right) \qquad (8)$$

when $\mathbf{G}_\parallel \neq \mathbf{0}$ and $G_z \neq 0$,

$$f_G = f_C \cdot S_z(H/2) + \overline{f}_{pc}\cdot S_{xy}(r_0)\cdot\left(S_z(l/2) - S_z(H/2)\right) \qquad (9)$$

when $\mathbf{G}_\parallel = \mathbf{0}$ and $G_z \neq 0$,

$$f_G = 2l^{-1}Hf_C + 2l^{-1}h(f_A - f_B)S_{xy}(r_0) \qquad (10)$$

when $\mathbf{G}_\parallel \neq \mathbf{0}$ and $G_z = 0$, and

$$f_G = 2l^{-1}Hf_C + 2l^{-1}h\overline{f}_{pc} \qquad (11)$$

when $\mathbf{G}_\parallel = \mathbf{0}$ and $G_z = 0$. In the above expressions, r_0 is the radius of the inclusions in the phononic plate, and

$$\overline{f}_{pc} = \frac{\pi r_0^2}{A_c}f_A + \left(1 - \frac{\pi r_0^2}{A_c}\right)f_B, \qquad (12)$$

$$S_{xy}(r_0) = \frac{2\pi r_0^2}{A_c}\frac{J_1(G_\parallel r_0)}{G_\parallel r_0} \qquad (13)$$

for a square lattice,

$$S_{xy}(r_0) = \frac{2\pi r_0^2}{A_c}\frac{J_1(G_\parallel r_0)}{G_\parallel r_0}\cos(G_y a) \qquad (13)$$

for a honeycomb lattice, and

$$S_z(z) = \frac{2z}{l}\frac{\sin(G_z z)}{G_z z} \qquad (14)$$

where A_c is the area on the *x-y* plane of a unit cell of the phononic plate, *a* is the distance between the centers of two nearest cylinders which is referred to as the lattice constant of a honeycomb lattice, and J_1 is the Bessel function of the first kind.

Finally, the eigenfrequency of the phononic plate mode can be solved by examining the condition

$$\det(\mathbf{L}) = 0 \qquad (14)$$

In the following calculations, we will consider two kinds of lattices that can open up full acoustic band gaps for an air-solid phononic crystal: square lattice and honeycomb lattice (as shown in Fig. 2).

(a)   (b)
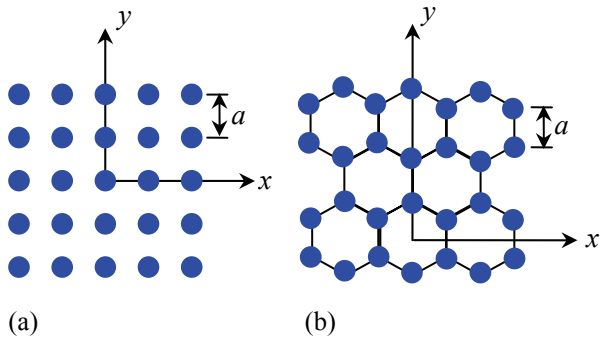
FIG. 2 Square lattice and honeycomb lattice and their corresponding definition of lattice constant.

2.2 Finite element method

In this study, analyses by using the finite element method is employed in order to compare the results obtained from the full 3D PWE method. We use the COMSOL MULTIPHYSICS commercial software to carry out the calculations of FEM. In the FEM model, a unit cell of the phononic-crystal plate is constructed, and, according to the Bloch theorem, the mechanical displacement field and electric potential of a monochromatic wave obey the following conditions on the boundary of the unit cell

$$u_j\left(\mathbf{r}+\mathbf{R}_{mp}\right)=u_j\left(\mathbf{r}\right)\exp\left(i\mathbf{k}\cdot\mathbf{R}_{mp}\right) \tag{15}$$

$$\phi\left(\mathbf{r}+\mathbf{R}_{mp}\right)=\phi\left(\mathbf{r}\right)\exp\left(i\mathbf{k}\cdot\mathbf{R}_{mp}\right) \tag{16}$$

where $\mathbf{R}_{mp}$ is a vector displaced by a 2D period of the lattice multiplied by an arbitrary pair of integers (m, p) in the spatial position, and $\mathbf{k}$ is the Bloch wave vector confined in the first Brillouin zone. With the conditions (15) and (16) applied to the unit cell, the eigenfrequency is then obtained by solving the piezoelectric wave problem of the model. Examples of the meshed unit cells of the phononic-crystal plates with square and honeycomb lattices are shown in Fig. 3, respectively.

(a)   (b)
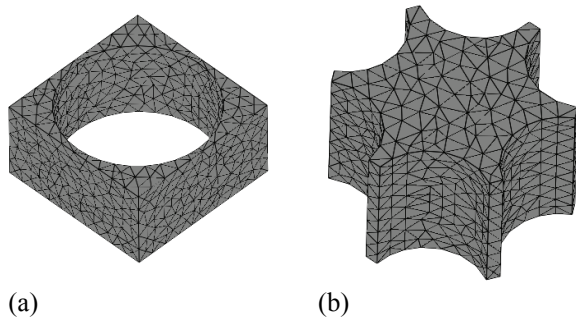
FIG. 3 Examples of the meshed unit cells of the phononic-crystal plates with the (a) square lattice and (b) honeycomb lattice in the FEM models.

3 Zinc-Oxide Phononic Crystal Plate

3.1 Acoustic band structures

We consider phononic-crystal plate consisting of a periodic air-hole array in a ZnO film. The material constants of ZnO used in all the calculations are listed as follows: ρ =5680 kg/m³, c_{11}=209.7GPa, c_{33}=210.9GPa, c_{44}=42.47GPa, c_{12}= 121.1Gpa, c_{13}=105.1Gpa, e_{15}=-0.48 C/m², e_{31}=-0.573 C/m², e_{33}=1.32 C/m², ε_{11} =75.7pF/m, ε_{33} =90.3pF/m.

(a)

(b)
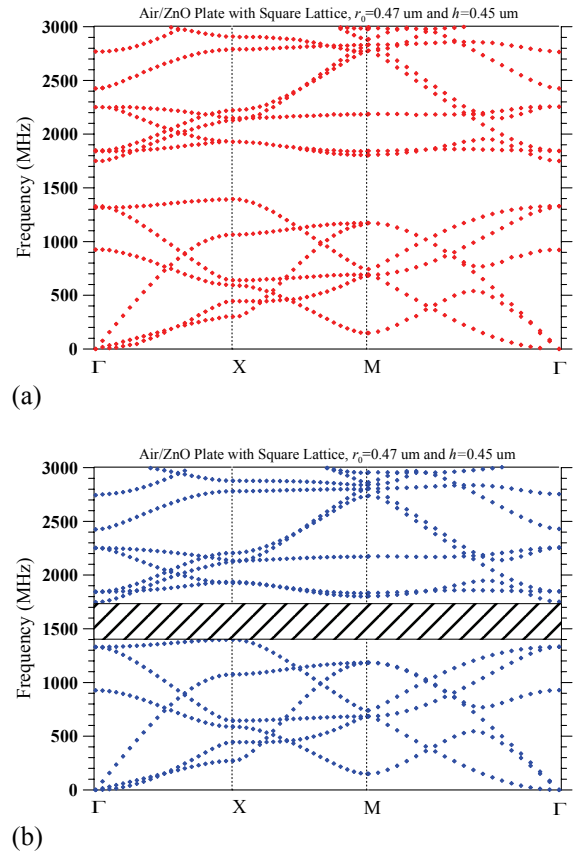
FIG. 4 Acoustic band structures of waves in phononic-crystal plates composed of a square-lattice air-hole array in a zinc oxide film. (a) PWE method. (b) FEM model.

Figure 4(a) and (b) show the acoustic band structures of ZnO phononic-crystal plate with a square lattice calculated by using the full 3D PWE method and FEM model, respectively. The lattice constant a is 1.00um. The radius of the air hole and plate thickness are r_0=0.47um and h=0.45um, respectively. The filling ratio of air is, therefore, F=0.694. Moreover, the thickness of the uniform vacuum layer assumed in the PWE calculation is 2.00um, which is enough to segregate the influences of the waves from the neighboring phononic plates. In the figures, the results by the two methods exhibit good agreement. In the full 3D PWE method, 81 Fourier terms in the expansions (i.e., 81 reciprocal lattice vectors or plane waves) are used in the 2D plane (i.e., *x-y* plane), and 5 plane waves are used along the *z*-direction. In the FEM model, 3643 tetrahedral elements are meshed for the unit cell. The full acoustic band gap is in the frequency range from 1.4GHz to 1.75GHz. The relative band-gap width, therefore, is about 22%. Figure 5 shows the vibrations of band-edge modes at the lower-edge (i.e.,

1397 MHz at X point) and upper-edge (i.e., 1750 MHz at Γ point) frequencies of the full band gap. At the lower-edge frequency, the most of the energy is localized on the up and down surfaces of the plate; however, at the upper-edge frequency, the energy is concentrated in the four ribs of the structure.

(a)

(b)
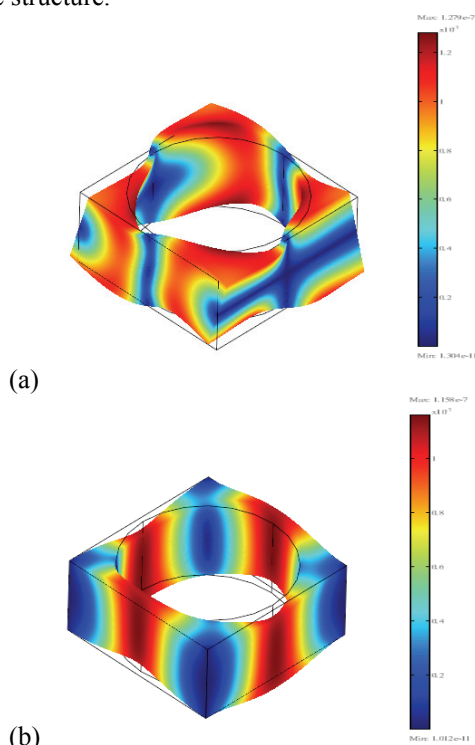
FIG. 5 Band-edge plate modes. (a) The mode at 1397 MHz of the lower edge and (b) the mode at 1750 MHz of the upper edge of the full band gap of the square lattice.

Figure 6 shows the acoustic band structure for the case with a honeycomb lattice calculated by the FEM model with about 6500 tetrahedral elements meshed. For this plate, the lattice constant is a=1.00 um, the radius of air hole is r_0=0.45 um (F= 0.490), and the plate thickness h=1.00 um. A wide full band gap ranges from 0.8GHz to 1.16GHz. The relative band-gap width is about 36.7%. Figure 7 shows the vibrations of band-edge modes at the lower-edge (i.e., 801 MHz at Γ point) and upper-edge (i.e., 1187 MHz at K point) frequencies of the full band gap. At the lower-edge frequency, the most energy is localized on the up and down surfaces of the plate; however, at the upper-edge frequency, the energy is concentrated in two of the ribs of the structure.
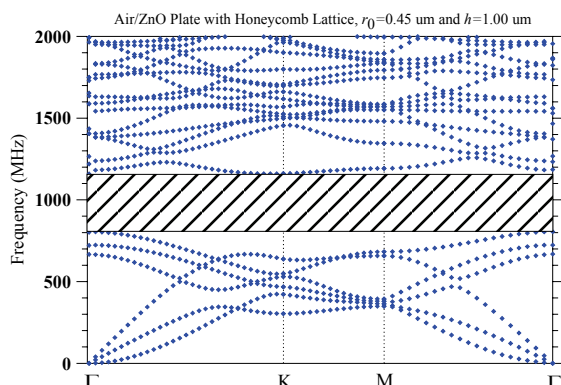
FIG. 6 Acoustic band structure of waves in the zinc-oxide phononic-crystal plate with a honeycomb-lattice.

(a)

(b)
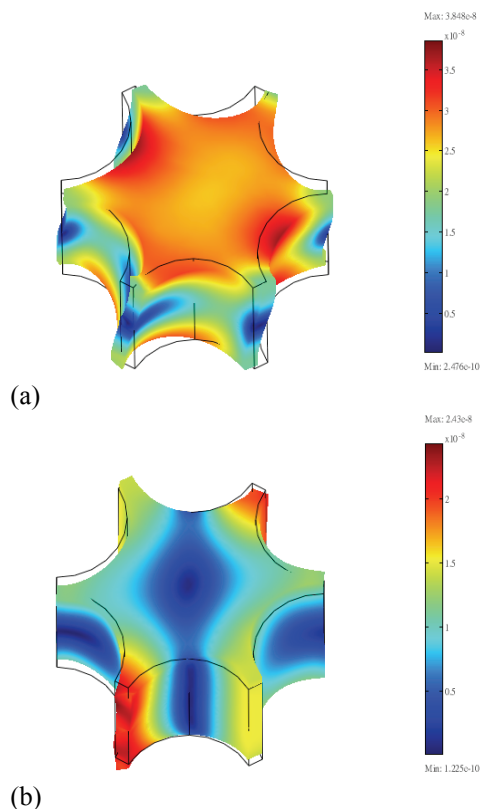
FIG. 7 Band-edge plate modes. (a) The mode at 801 MHz of the lower edge and (b) the mode at 1187 MHz of the upper edge of the full band gap of the honeycomb lattice.

3.2   Effect of plate thickness

For a phononic-crystal plate structure, the plate thickness can also be dominated the open and width of the full band gaps. Figures 8(a) and (b) show the distributions of the full band gaps as a function of plate thickness h for the square lattice and honeycomb lattice, respectively. For the square lattice, the lattice constant and radius of holes are 1.00um and 0.47um, respectively, and for the honeycomb lattice, the lattice constant and radius of air holes are 1.00um and 0.45um, respectively. The calculations are based on the FEM model. Note that more meshed elements in the model are needed to obtain a convergent result when the plate thickness is increased. In Fig. 8(a), two regions of band gaps are in the frequency-thickness diagram for the square lattice. The frequencies of band gaps are distributing in the range form 1180MHz to 1840MHz. This frequency range is in between the fundamental plate modes and their first folded bands, and the full band gaps is affect by the folded bands of the flexural mode and the modes with a cutoff frequency that are shifted by changing the plate thickness. In Fig. 8(b), the distributions of the full band gaps are much more complicated for the honeycomb lattice. The region of the full band gap is divided into five areas by shift of the flexural bands and cutoff-frequency modes as the plate thickness changes in the diagram. Moreover, the band-gap frequencies are in the lower frequency range (about from 790MHz to 1420MHz) than that of the square lattice in spite of their same value of the lattice constant a in the corresponding plate thickness.

(a)

(b)
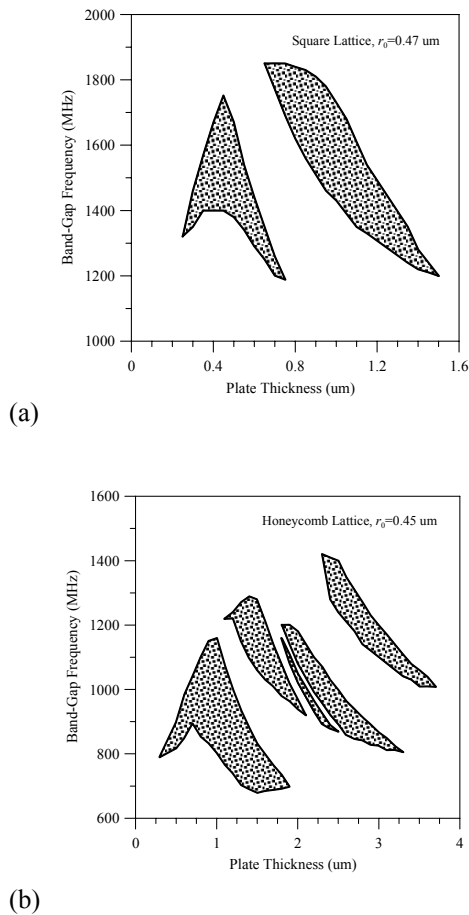
FIG. 8 Band-gap distributions as a function of the plate thickness h. (a) Square lattice with r_0=0.47um; (b) honeycomb lattice with r_0=0.45um.

Conclusion

By utilizing the full 3D PWE method and FEM, we studied the acoustic band structures and full band gaps of acoustic waves propagating in piezoelectric phononic crystal plate. The plate is composed of a periodic air-hole array in a ZnO film. The revised formulation of PWE method applied to the plate structure is derived by considering an imaginary 3D periodic structure that stacks the phononic plates and uniform vacuum layers alternatively. In the plates, two lattices are considered in this study, i.e., the square lattice and honeycomb lattice in which both exhibit wide full band gaps according to the theoretical calculations. Comparison of the calculated results respectively by the PWE method and FEM model also shows good agreement. Finally the effect of the plate thickness on the full band gaps is discussed for the two lattices, respectively. For the square lattice, the band-gap frequencies appear at higher frequency range, while the full band gaps are in the lower frequency ranges for the honeycomb lattice.

Acknowledgments

References

[1] J.-H Sun and T.-T. Wu, "Propagation of surface acoustic waves through sharply bent two-dimensional phononic crystal waveguides using a finite-difference time-domain method," *Phys. Rev. B* 74, 174305 (2006).

[2] Y. Pennec, B. Djafari-Rouhani, J. O. Vasseur, A. Khelif, and P. A. Deymier, "Tunable filtering and demultiplexing in phononic crystal with hollow cylinders," *Phys. Rev. B* 69, 046608 (2004).

[3] Y. Tanaka and S. Tamura, "Surface acoustic waves in two-dimensional periodic elastic structures," *Phys. Rev. B* 58, 7958-7965 (1998).

[4] T.-T. Wu, J.-C. Hsu, and Z.-G Huang, "Band gaps and the electromechanical coupling coefficient of a surface acoustic wave in a two-dimensional piezoelectric phononic crystal," *Phys. Rev. B* 71, 064303 (2005).

[5] J.-C. Hsu and T.-T. Wu, "Bleustein-Gulyaev-Shimizu surface acoustic waves in two-dimensional piezoelectric phononic crystals," *IEEE Trans. Ultrason. Ferroelectr. Freq. Control* 53, 1169-1176 (2006).

[6] X. Zhang, T. Jackson, E. Lafond, P. Deymier, and J. Vasseur, "Evidence of surface acoustic wave band gaps in the phononic crystals created on thin plates," *Appl. Phys. Lett.* 88, 041911 (2004).

[7] J.-C. Hsu and T.-T. Wu, "Efficient formulation for band-structure calculations of two-dimensional phononic-crystal plates," *Phys. Rev. B* 74, 144303 (2006).

[8] A. Khelif, B. Aoubiza, S. Mohammadi, A. Adibi, and V. Laude, "Complete band gaps in two-dimensional phononic crystal slabs," *Phys. Rev. E* 74, 046610 (2006).

[9] J.-C. Hsu and T.-T. Wu, "Lamb waves in binary locally resonant phononic plates with two-dimensional lattices," *Appl. Phys. Lett.* 90, 201904 (2007).

[10] Y. Tanaka, Y. Tomoyasu, and S. Tamura, "Band structure of acoustic waves in phononic lattices: Two-dimensional composites with large acoustic mismatch," *Phys. Rev. B* 62, 7387-7392 (2000).

[11] M. M. Sigalas and E. N. Economou, "Elastic waves in plates with periodically placed inclusions," *J. Appl. Phys.* 75, 2845-2850 (1994).

[12] M. Wilm, S. Ballandras, V. Laude, and T. Pastureaud, "A full 3D plane-wave-expansion model for 1-3 piezoelectric composite structures," *J. Acoust. Soc. Amer.* 112, 943-952 (2002).

[13] J. O. Vasseur, P. A. Deymier, B. Djafari-Rouhani, Y. Pennec, and A-C. Hladky-Hennion, "Absolute forbidden bands and waveguiding in two-dimensional phononic crystal plate," *Phys. Rev. B* 77, 085415 (2008).

[14] Z. Hou and B. M. Assouar, "Modeling of Lamb wave propagation in plate with two-dimensional phononic crystal layer coated on uniform substrate using plane-wave-expansion method", *Phys. Lett. A* 372, 2091-2097 (2008)